Artificial antenna systems

GION CALZAFERRI
Department of Chemistry and Biochemistry, University of Bern,
Freiestrasse 3 CH-3000 Bern, Switzerland

Abstract. The work describes experimental and theoretical results on the water oxidation in absence of an externally added potential, on the charge transport in organized microporous media and on the transport of excitation energy in an antenna system. Water oxidation to O_2 takes place at the solid/water phase boundary of a thin AgCl layer in the presence of a small excess of Ag^+. This water oxidation step shows self-sensitization as the reaction proceeds, the sensitivity is extended from the near-UV-visible towards the red range. The quantum yield per redox equivalent for O_2 evolution upon illumination with near UV light (340–390 nm) is ~ 0.8 and it is the same upon illumination with blue light (420–480 nm). In the green range it is ~ 0.5. We discuss parameters controlling these reactions. Zeolite microcrystals are investigated as hosts for supramolecular organization of clusters, complexes and molecules. The possibility to arrange zeolite microcrystals of good quality and narrow size distribution as dense monograin layers on different types of substrates allows the discovery of specific properties. In the present context, three functionalities are of special importance intrazeolite ion transport, intrazeolite charge transport and intrazeolite excitation energy transport. All of them have been clearly demonstrated experimentally although there are still some controversies going on. Highly concentrated dyes have the tendency to form aggregates which generally show very fast radiationless decay. In natural antenna systems the formation of aggregates is prevented by fencing the chlorophyll molecules in polypeptide cages. A similar approach is possible by enclosing dyes inside a microporous material such that the volume of the cages and channels is able to uptake monomers only, but not aggregates. We know a number of materials bearing linear channels running through the whole microcrystal which allow the formation of highly anisotropic, monomeric dye assemblies. A few cases based on zeolite L as a host and the cationic dye molecules pyronine and oxonine have been investigated experimentally to some extent for this purpose. While the molecules can penetrate the channels, the geometrical constraints of this system excludes aggregation and therefore self-quenching up to very high concentrations, namely 0.2 M. Microcrystals with cylinder morphology and a size in the range of 100 nm have been found to be optimal for realizing collection efficiencies in order of 99%.

Keywords. Dye molecules; zeolite microcrystals; photochemical water splitting device; efficient antenna device.

1. Introduction

An important aim of photochemistry is to discover or to design structurally organized and functionally integrated artificial systems which are capable of elaborating the energy and information input of photons to perform functions which are useful for energy or information purposes. In natural photosynthesis, light is absorbed by an antenna system of a few hundred chlorophyll molecules arranged in a protein environment which allows a fast energy transfer from an electronically excited molecule to

unexcited neighbour molecules in a way that the excitation energy reaches the reaction centre with high probability. Trapping occurs there. An artificial antenna system is an organized multi-component arrangement in which several chromophoric molecular species absorb the incident light and channel the excitation energy (not charges) to a common acceptor component[1]. Experiments for controlled transport of excitation energy through thin layers based on Langumuir–Blodgett films have been described many years ago by Kuhn *et al*[2]. Some sensitization processes in silver halide photographic materials and also the "dyes, complexes and thin layers in sensitization solar cells"[3] bear in some cases aspects of artificial antenna systems[4].

An overview of relevant processes in a photochemical water splitting device in which the oxidation of water to oxygen and its reduction to hydrogen are separated by a membrane is illustrated on the upper part of figure 1. Water oxidation takes place at the solid/liquid phase boundary. An antenna absorbs and transports the excitation energy to an oxidizing species which is itself reduced. Re-oxidation takes place by electron transport to the membrane and then through it, to the reducing side. Using a mediator for transporting the electron to the reducing species at the phase boundary where hydrogen evolution takes place is an interesting possibility. Realizing such a device in which several parts play well together is the aim but it is indeed a demanding task. A conceptual simplification can be made by substituting the membrane temporarily by two electrodes as illustrated on the lower part of figure 1. This allows the study of the oxidative and the reductive parts separately. We refer to references[5] and [6] for recent reviews on photochemical water splitting.

We have focused on three problems, the water oxidation in the absence of an externally added potential, the charge transport in an organized microporous media
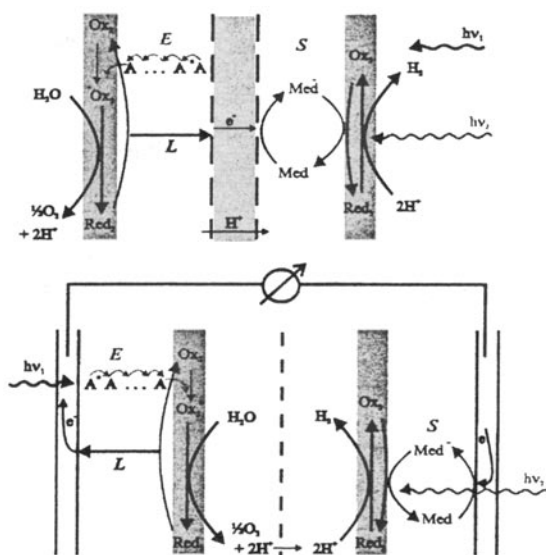

Figure 1. Overview of relevant processes in a photochemical water splitting device. Upper part: The oxidation of water to oxygen and its reduction to hydrogen are separated by a membrane. Lower part: simplification by substituting the membrane by two electrodes. *E* indicates migration of excitation energy, *L* indicates charge transport and *S* indicates charge transport by a mediator.

and the transport of excitation energy in an antenna system. I will start by discussing the photochemical oxidation of water on Ag^+ containing systems and the self-sensitization taking place during this reaction. A few remarks on zeolite microcrystals as hosts for supramolecular organization of clusters, complexes and molecules will then lead to an actually promising project concerning the energy transfer between dye molecules in the nanopores hexagonal microcrystals.

We became interested in the water oxidizing ability of Ag^+–A zeolite containing systems when we observed that self-sensitization takes place: as the reaction proceeds, the sensitivity is extended from near-UV-visible wavelengths toward the red range[7]. We recently examined the influence of Cl^- on this reaction[8] and we found that thin AgCl layers evolve O_2 in the presence of a small excess of Ag^+ ions. This system shows the same type of self-sensitization as we reported earlier. The quantum yield for O_2 evolution upon illumination with near UV light is ~ 0.8 and it is the same upon illumination with blue light (420–480 nm). In the green range (500–540 nm) it is ~ 0.5. A question to be discussed is whether the action of the chromophores responsible for the self-sensitization can be understood in terms of an antenna or if they act as reaction centre themselves. If this system is to become useful in a regenerative way, the reduced silver species must be reoxidized to silver cations in a completely reversible process.

Zeolite microcrystals offer the possibility to act as hosts for supramolecular organization of clusters, complexes and molecules. One can imagine that such an organized system should allow to design precise and reversible functionalities which have the potential to become useful in a solar energy conversion system. As an example, the electronic structure of silver zeolite *A* is very interesting and offers possibilities for building new devices. Very different systems are obtained by intercalating strongly luminescent organic dyes such as pyronine, oxonine and others into the channels of zeolite *L* and other hexagonal zeolites with channel structure. The geometrical constraints of this system excludes aggregation and therefore self-quenching up to very high concentrations of about 0.2 M. The highly anisotropic arrangement realized in such systems has been used to study possibilities for building an efficient light harvesting antenna system based on Förster energy transfer[9]. The principle of such a device is illustrated in figure 2. We have shown that its pronounced anisotropy strongly favours the probability to reach a trap located in the middle of one of the ends of the cylinder shaped microcrystals[10].

2. Photochemical oxidation of water to oxygen and the early days of photography

The photochemical oxidation of water to oxygen is a four-electron process. It is therefore intrinsically difficult to understand. In green plants it is assumed to proceed via a manganese complex system but despite intense research, many open questions remain to be answered[11]. Remarkably interesting chemistry has been developed in attempts to mimic the natural systems but it seems that there is still a very long way to go before we reach this goal.

The photographing papers of Henry Fox Talbot, prepared around 1834, were made by first soaking in sodium chloride solution and then brushing with an excess of silver nitrate solution. The key to success was the observation that the paper was more sensitive to light where there was a deficiency of $NaCl$[12]. We recently reported that the photochemical oxygen evolution of a silver chloride containing zeolite in presence of water depends on the added amount of Cl^-[13,8]. We found that there is a maximum of O_2 production where there is a deficiency of Cl^- with respect to stoichiometric AgCl.
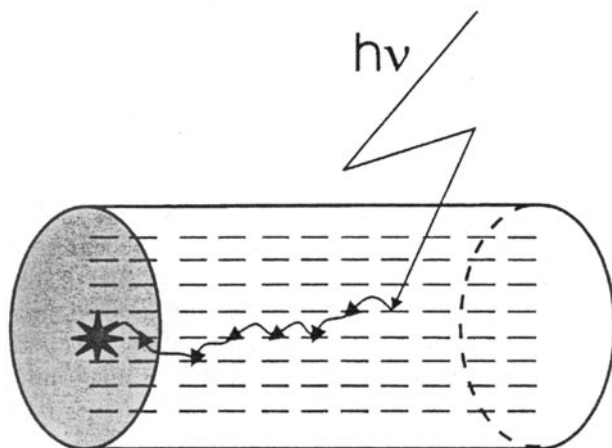
Figure 2. An artificial antenna system. Light is collected absorbed by the dye molecules indicated as bars. The direction of the transition of the first electronic transition coincides with the axis of the cylinder. The excitation then migrates along the linearly arranged dye molecules until it reaches the trap, marked by a star, as indicated by the arrows. An important aspect of this device is its pronounced anisotropy concerning the excitation energy migration.

I became aware of the fact that our observations parallel those made by Talbot 160 years ago, when I followed a paper presented by Dr Ware at the IS&T's 48th Annual Meeting in Washington 1995[14]. Since then, I assume that the first photographic papers of Talbot were based on the ability of silver chloride to oxidize water to oxygen with high quantum yield in presence of an excess of Ag^+ ions. These early silver photographs were not fixed by thiosulphate but were simply *stabilized* by an excess of halide ions. Talbot published an article entitled *The Nature of Light* in 1835 in which he described an observation that resembles the *latent image* formation which made silver photography so successful and which was close to the *self-sensitization process* for the photochemical oxidation of water, discovered by us a few years ago[13,8,7]. Talbot did not understand what he had observed but the description of the phenomenon is remarkably precise. He writes, "... A sheet of paper was moistened with a solution of nitrate of silver, a substance which, it is well known, is capable of being blackened by the influence of solar light. Half of the paper was covered, and half exposed to sunshine; but owing to it being a dull day in the winter season, no effect was produced. After several minutes the paper was removed, and being examined, showed hardly any perceptible difference between the part that had been covered and that which had been exposed to the sun..It was then removed to another room, where the sun does not shine in the winter season, and accidentally exposed to daylight. Some hours afterwards I was surprised to find that the paper had become partially darkened, and that the dark part was that which had been previously but ineffectually exposed to the sunshine, while the other part still retained much of its original whiteness. This anomalous fact, of which I could find no explanation at the time, appears to me now to be closely connected with what I have advanced as a probable cause of phosphorescence. ..."

The three essential observations made by Talbot that (i) his paper was more sensitive to light where there was a deficiency of NaCl; (ii) that his paper could be *stabilized* by an

excess of Cl⁻ under optimized conditions and (iii) that it could be sensitized by moderate illumination parallel important observations we have made when studying the ability of Ag⁺ containing systems in the presence of a deficiency of Cl⁻ to photo oxidize water to oxygen[13,8].

Baur and Rebmann seem to be the first to report on minor O_2 evolution from water on UV illumination of AgCl[15]. An article of Vogel dating back to 1863 which is sometimes wrongly referred as to be the first report on photochemical O_2 production from AgCl does not contain any hints on photochemical O_2 evolution[16]. Vogel was probably, however, the first to demonstrate the photochemical oxidation of Cl⁻ to Cl_2 in an aqueous silver chloride system which at the same time became more acidic on illumination with sunlight under certain conditions. In a study of the *p*H dependence of the photochemical properties of AgCl and of Ag⁺−A zeolite, both in the presence of a large excess of Cl⁻, we have shown that, under acidic conditions, Cl_2 is evolved with a significant quantum yield and O_2 signals appear only in the strongly alkaline region. We also found that this system shows self-sensitization. Based on these observations we built an {Ag⁺/AgCl‖Cl⁻/Cl_2} photogalvanic cell with an open circuit potential of 1.05 V, but poor power/voltage behaviour[17].

Metzner and co-workers reinvestigated the experiments of Baur and Rebmann in an attempt to contribute to the understanding of the ability of the natural photosystem II to evolve oxygen. They observed significant O_2 evolution from AgCl suspensions containing an excess of Ag⁺ showing a maximum of sensitivity at about *p*H5[18]. Chandrasekaran and Thomas observed photochemical oxidation of water with AgCl in the presence of an excess of Ag⁺ with a low quantum yield but they did not try to optimize the conditions[19]. They assumed that OH-radicals play a role in this process but no evidence was advanced to support this. We have good reason to beleive that these radicals do not play any role in the photochemical oxidation of water by AgCl/Ag⁺ systems. This is consistent with the finding of Taube and Bray that OH-radicals react which chloride to form Cl-radicals[20].

We conclude that the observations (i) and (ii) of Talbot were repeated with partial success in a number of labroatories over several decades by experimentalists not being aware of it, however.

We became interested in the water oxidizing ability of Ag⁺−A zeolite containing systems, contaminated with some AgCl, when we observed that a system that has never been exposed to near UV light ($\sim$370 nm) is insensitive to visible light but that it becomes sensititve and is capable to photo-oxidize water to O_2 in the whole visible range with a limit between 600 to 700 nm with high quantum yield under optimized conditions. We named this a *self-sensitization process*, because as the reaction proceeds, the sensitivity is extended from the near UV wavelengths towards the reaction range[7,13,8]. The self-sensitization parallels the observation (iii) described by Talbot 1835.

Our present knowledge on the ability of Ag⁺ containing systems in the presence of an optimal amount of Cl⁻ to photo-oxidize water to oxygen can be summarized as follows,

(1) AgCl/Ag⁺ on zeolites, on SnO_2, on glass, on silver, and on other substrates is able to photo-oxidize water to O_2 according to the following stoichiometry,

$$[nAg^+, mAgCl] + \frac{r}{2}H_2O \xrightarrow{h\nu} [(n-r)Ag^+, mAgCl, rAg^0] + rH^+ + \frac{r}{4}O_2.$$
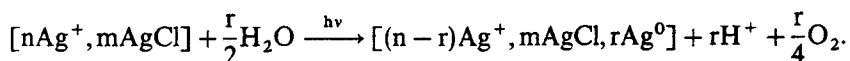
Important parameters are: the Ag⁺ to Cl⁻ ratio, the *p*H, the wavelength and the light intensity.

(2)   Self -sensitzation occurs under all conditions investigated. A system that has never been exposed to light is insensitive to the visible part of the spectrum. After it has been once irradiated in the near UV it becomes sensitive and is capable to photo-oxidize water in the whole visible range with a lower limit between 600 and 700 nm. Once the system has been sensitized, the near UV irradiation can be omitted.

(3)   The oxygen evolution rate is not linear at low light intensities. It becomes linear above about $300 \,\mu W/cm^2$. This is qualitatively the same at all wavelengths we have investigated, namely in the near UV, the blue and the green range. The quantum yield was measured to be at least 0·8 for near UV and for blue light and at least 0·5 for green light, in the linear range.

(4)   The *pH* of maximum oxygen evolution depends on the composition of the system. For an AgCl layer with an excess of about $10^{-3} M Ag^+$ it is at approximately *pH* 4. In case of AgCl on Ag^+–A zeolite it is around *pH* 6 and on mordenite it is in the alkaline region. This means that optimization for a specific application is feasible to a certain extent. In presence of a small excess of Cl^- the system becomes insensitive to daylight while at a large excess chlorine evolution is observed under acidic conditions with substantial quantum yield and oxygen can be detected with low yield only under alkaline conditions.

(5)   We have recently carried out experiments at the gas/solid interface. No oxygen evolution was observed at $AgCl/Ag^+$ layers but significant oxygen signals and also self-sensitization were measured for AgCl deposited on Ag^+–A zeolite. An explanation for this could be that the $AgCl/Ag^+$ layers become immediately very acidic so that only tiny amounts of oxygen can be formed while the buffering capability of the zeolite framework helps to maintain favourable conditions for the oxidation of water in $AgCl/Ag^+$–A zeolite samples[21].

Based on these observation we deduce a reaction mechanism of the photochemical oxygen evolution which also takes into account the very different behaviour of $AgCl/Ag^+$ $AgCl/Cl^-$[8].

- Light absorption proceeds via a LMCT transition in which an adsorbed silver atom and an adsorbed chlorine radical are formed at the surface. This can also be described as *electron-hole pair* formation. The chlorine radical can be understood as a surface species (s) and the silver atom can be understood as an interstitial (i) surface species.

- (A) $AgCl + h\nu \xrightarrow{\text{charge transfer transition}} Ag^{\cdot}_{s,i} + Cl^{\cdot}_{s}$
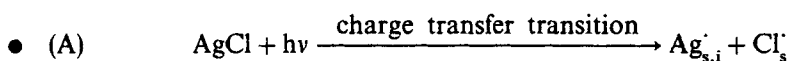
- Any recombination is a loss process.
- Two radicals combine to form Cl_2. Chlorine evolution has been measured in a number of experiments, see e.g.[17].

- (B) $2Cl^{\cdot}_{s} \longrightarrow Cl_2$
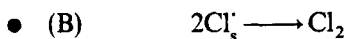
- At low *pH* Cl_2 is stable and can be collected. In less acidic conditions it reacts with water to form hypochloric acid.

- (C) $Cl_2 + H_2O \rightleftharpoons HOCl + H^+ + Cl^-$
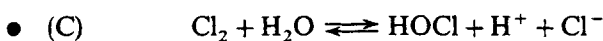
- This reaction is supported by an excess of Ag^+ which captures the Cl^- and shifts the equilibrium to the right.

- (D) $\qquad$ $Cl^- + Ag_s^+ \rightleftharpoons AgCl_s$

- HOCl acid is a weak acid with a pK_a value of 7·58.

- (E) $\qquad$ $HOCl + OH^- \rightleftharpoons OCl^- + H_2O$

- HOCl and OCl^- are rather stable under many conditions. However, silver species catalyse the decomposition of HOCl to oxygen, protons and Cl^- according to,

- (F) $\qquad$ $2HOCl \xrightarrow{AG^+} O_2 + 2H^+ + 2Cl^-$

- Step (F) can be tested easily by adding silver nitrate to a hypochloric acid solution which causes rapid oxygen evolution.
- The interstitial silver atoms form clusters of yet unknown size and charge according to equation (G), as can easily be observed by the colour change taking place.

- (G) $\qquad$ $nAg_{s,i}^{\cdot} + mAg^+ \xrightarrow{\text{cluster growth}} [Ag]_{n+m}^{m+}$

- These clusters act as colour centres, responsible for the self-sensitization.

Step (B) explains why, with acidic solutions and an excess of Cl^-, chlorine formation is observed, while step (F) explains the oxygen evolution in case of an excess of Ag^+ and at medium pH. At low light intensities, we observed a non-liner dependence of the O_2 evolution rate on the light intensity which changes into a linear dependence above about $300\,\mu W/cm^2$. Four redox equivalents have to be accumulated for the formation of one O_2 molecule. In the mechanism presented, this occurs in steps (B) and (F), where two partially oxidized species react with each other. It is reasonable to assume that recombination reactions play a more important role at low light intensities than at higher values, because the speed of step (B) depends crucially on the concentration of chlorine radicals. At low intensity the oxygen evolution rate is proportional to the square of the light intensity. The lifetime of the chlorine radicals can be estimated to be in the order of a few dozen micro seconds. This estimate is based on luminescence lifetime measurements. Above a critical light intensity the chlorine radical concentration is so high that losses become negligible.

It is satisfactory that the photochemical oxygen evolution on $AgCl/Ag^+$ systems can be explained as a sequence of simple one electron steps. The excess of Ag^+ needed for efficient oxygen evolution is due to a surface effect. The two different situations, excess of Ag^+ and excess of Cl^- in the system, can be sketched as shown in figure 3.

The reduced silver species must be oxidized to make the photochemical water oxidation useful for solar energy conversion.

$$[(n - r)Ag^+, mAgCl, rAg^0] \xrightarrow[\text{electrode or membrane}]{+ r\oplus} [nAg^+, mAgCl.$$
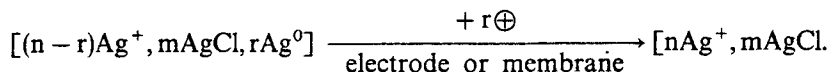
It is not difficult to reoxidize the photochemically produced Ag^0 completely to Ag^+. It is, however, difficult to design a completely reversible and stable system. The two complementary approaches illustrated in figure 1 can be tried. One of them is to design a photo electrochemical cell in which the reduced silver is reoxidized electrochemically and in which hydrogen is evolved at an appropriate (photochemically driven)
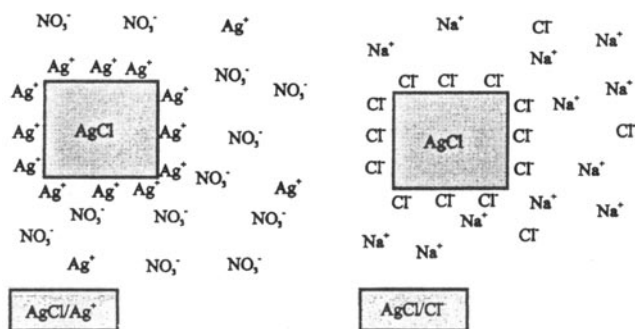
Figure 3. Surface of AgCl for different concentrations of Ag^+ and Cl^- ions in the solution. Left: When Ag^+ is in excess the AgCl carries an excess silver ions at its surface and the double layer is completed by the counter ion, nitrate; this is the $AgCl/Ag^+$ case. Right: When the halide ion is in excess the remaining AgCl adsorbs an excess halide ions on its surface and a sheath of Na^+ ions completes the electrical double layer; this is the $AgCl/Cl^-$ case.

counter-electrode. An intellectually more satisfactory but in principle also more difficult approach is to realize a completely reversible system by dividing it into an oxidative and a reductive half cell via a membrane[22]. Zeolite based systems are attractive for both approaches.
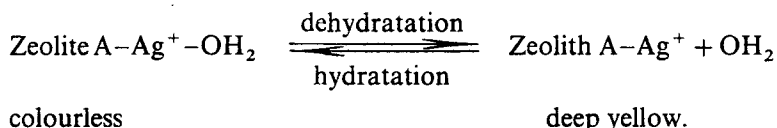
3.   Zeolite microcrystals as hosts for supramolecular organization of clusters, complexes and molecules

Zeolite microcrystals can act as hosts for supramolecular organization of clusters complexes and molecules, see e.g.[23,24]. They offer possibilities to design precise and reversible functionalities which have the potential to become useful in a solar energy conversion system because in favourable cases very stable materials have been obtained. The possibility to arrange zeolite microcrystals of good quality and narrow size distribution as dense monograin layers on different types of substrates allows us to achieve specific properties[25]. In the present context three functionalities are of special importance, intrazeolite ion transport, intrazeolite charge transport and intrazeolite excitation energy transport. All of them have been clearly demonstrated experimentally although there are still some controversies going on. The zeolite acts as a host in each case mentioned. It is not actively involved in the corresponding processes, but provides the necessary geometrical and chemical environment. One of the difficulties in this field is that the materials used are often poorly characterized and do not correspond to what the experimentalists assume to have in their hands[26,27]. The zeolite community has made it difficult for newcomers to synthesize or to obtain the material they need to have. But this unpleasant situation is improving rapidly.

Silver zeolite A is a good example to illustrate some difficulties but especially the appealing properties of such systems. It was assumed that the zeolite is important in the photochemical oxidation of water with visible light observed in Ag^+–A zeolite system. This turned out not to be the case in presence of liquid water[8,28] but the zeolite ion exchange properties where found to play an important role in experiments at the solid/gas interface, however, as discussed in the previous section.

In-situ spectroscopy on well defined monograin layers and quantumchemical calculations on systems containing several hundred atoms have provided new insight. Rálek *et al* reported in 1962 that Ag^+–A zeolites turn from white over yellow to full yellow-red under dehydration at elevated temperature and that this colour change is reversible under rehydration[29]. These colour changes were repeated and discussed by a number of authors and the explanations for their occurence range from charge transfer interactions between the Ag^+ ions and the zeolite framework oxygen, responsible for the yellow colour, to multistep autoreductive processes involving framework oxygen and formation of partially reduced silver clusters. This discussion has been reviewed by Sun and Seff[30]. We have observed that the yellow colour can be observed by evacuating thin Ag^+–A zeolite layers at room temperature.

After adding a little degassed water via the vacuum system, the samples turned to white again within a fraction of seconds. This was reproduced several times over three days and no permanent changes could be observed. Addition of dry oxygen to the yellow samples did not have any visible effect. Based on this information and on quantumchemical calculations we concluded that the yellow colour of the evacuated Ag^+–A zeolite layers can be attributed to a LMCT charge transfer from the zeolite framework oxygen to the silver ions and that the colour change can be described simply as a dehydratation/hydratation process of the Ag^+ in the zeolite[31]:

$$\text{Zeolite A–Ag}^+\text{–OH}_2 \underset{\text{hydratation}}{\overset{\text{dehydratation}}{\rightleftharpoons}} \text{Zeolith A–Ag}^+ + \text{OH}_2$$

colourless   deep yellow.

More detailed experimental and theoretical studies on Ag_n^{m+} clusters in the zeolite A cavities has lead to the interpretation explained in figure 4. In the upper part you see the development of the Ag(5s)-type levels of the silver species in a zeolite. The lowest and the highest Ag(5s)-type levels are shown. All of them are embedded between the HOMO region of the zeolite, which consists of oxygen lone pairs denoted as (> O|), and its LUMO region lying at -2 to $0\,eV$ which is not shown. The Ag(5s)-type levels interact only weakly with levels belonging to the zeolite. The largest cluster in case of zeolite A consists of 6 silver atoms. The position of the cluster-HOMO depends on the charge of the cluster. It makes sense to name the lowest Ag(5s)-type level '*lowest-s-molecular orbital*' LOSMO, because of the special role it plays in the description of luminescence properties of such materials due to its position and due to the weak interaction of the Ag(5s)-type level with the zeolite framework.

The lower part of this view graph illustrates absorption/emission properties of a distorted Ag_6^+ cluster embedded in a zeolite framework. An electron is injected into the cluster from the zeolite-oxygen lone pair region via a LMCT transition. Emission can occur from all three doubly occupied Ag(5s)-type levels, the longest wavelength emission being of $>$ O| $\leftarrow$ LOSMO MLCT type. More details on these interesting observations will be published elsewhere[32].

Many different zeolite based materials have been reported. An interesting example is the $Ru(bpy)_3^{2+}$-Y zeolite which was discussed by Dutta two years ago at this conference[24]. We have shown that up to about 60% of the supercages can be filled with this complex, by the known '*ship-in-a-bottle*' syntheses procedures[26]. Our result is illustrated in figure 5. At higher loading an increasing amount of by-products corresponding formally to $Ru(bpy)_n(NH_3)_{6-2n}^{3+}$, $n < 3$, was found.
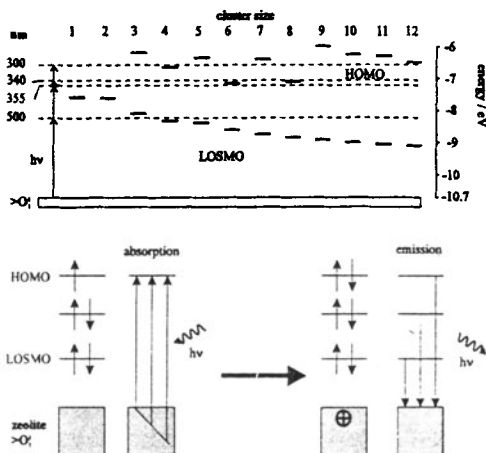
Figure 4. Electronic structure and electronic absorption/emission processes in silver zeolites. Upper part: Development of the Ag(5s)-type levels of the silver species in a zeolite. The lowest and the highest Ag(5s)-type levels are shown. All of them are embedded between the HOMO region of the zeolite, which consists of oxygen lone pairs denoted as ($>$O|). The position of the different cluster-HOMOs are indicated by a dashed line. It depends on the size and on the charge of the clusters. The lowest Ag(5s)-type level, the LOSMO, plays a special role in the description of luminescence properties of such materials. Lower part: Absorption/emission properties of a distorted Ag_6^+ cluster embedded in a zeolite framework. An electron is injected into the cluster from the zeolite-oxygen lone pair region via an LMCT transition. Emission is of MLCT type. It can occur from all three doubly occupied Ag(5s)-type levels, the longest wavelength emission being a $>$O| $\leftarrow$ LSOMO transition.
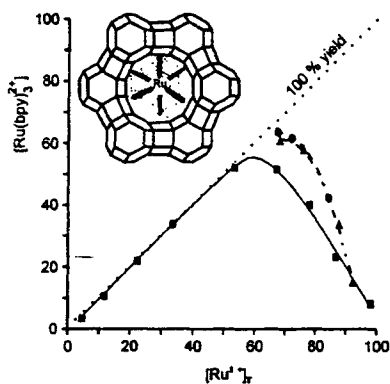

Figure 5. Analysis data for zeolites at different loadings. The loading $[Ru(bpy)2^{3+}]$ is drawn as a function of the total loading $[Ru^{2+}]_T$. A 100% value corresponds to a loading of one ruthenium/bpy complex per supercage. The samples at high loading were reacted with bpy a second time (triangles) and, in some cases, a third time (circles)[26].

Another interesting material which has been investigated by us and others is MV^{2+} in zeolite *Y*. This is the easiest case known so far to demonstrate intrazeolite charge transfer because a very pronounced and easy to understand dependence of the cyclic voltammogramms on the electrolyte cations was observed[33].

Very different systems are obtained by intercalating strongly luminescent organic dyes into the nanopores of hexagonal zeolites with channel structure. We discuss them in the next section.

4. Energy transfer between dye molecules in the channels of hexagonal microporous crystals.

From the natural antenna we deduce that highly concentrated monomeric dye molecules with a large Förster energy transfer radius and a high luminescence quantum yield in an ideal geometrical arrangement of optimal size are favourable conditions for realizing an efficient device as illustrated in figure 2. Dyes in high concentration usually have the tendency to form aggregates, which in general, show very fast radiationless decay. In natural antenna systems the formation of aggregates is prevented because the chlorophylls are fenced in polypeptide cages[34]. A similar approach is possible by enclosing dyes inside of a microporous material such that the volume of the cages and channels is able to uptake monomers only but not aggregates. Materials bearing linear channels running through a whole microcrystal allow the formation of highly anisotropic dye assemblies. Zeolites having such channels, large enough to uptake organic dye molecules, are especially attractive. Examples of such zeolites can be found in reference[35]. A few cases based on zeolite L as a host and the cationic dye molecules pyronine and oxonine have been investigated experimentally to some extent for this purpose[9]. Intercalation of thionine in zeolite L was found to be useful for learning about space filling properties and about isothermal ion exchange relevant in these studies[36]. Space filling models show that while the molecules can penetrate the channels, formation of dimers inside of them is not possible. The synthesis of zeolite L microcrystals with sizes ranging from 20 nm to 1 μm and with cylinder morphology and varying length to diameter ratio ranging from a disc to a cigar-like shape has recently been reported[37].

Gfeller and Calzaferri have carried out a theoretical study on energy transfer, energy migration, and trapping efficiencies of systems related to that illustrated in figure 2[10]. The basic assumptions used in these investigations can be summarized as follows. The antenna is built by dye molecules in hexagonally arranged linear channels as illustrated in figure 6. The primitive vector c corresponds to the channel axis while the primitive vectors a and b are perpendicular to it enclosing an angle of 60°. The channels run parallel to the central axis of the cylinder. The length and radius of the cylinder are l_{cyl} and r_{cyl} respectively. The theory is based on a few assumptions which are supported by experiments carried out on cationic dye molecules in zeolite L[9,36]. The description of the processes is simplified by referring to a large number of microcrystals with a narrow distribution of size and shape.

(a)   The dye molecules are positioned at sites fixed along the linear channels. The sites do not overlap. The length of a site is equal to an integral number u times the length c, so that one dye molecule fits into one site. The number u depends on the size of the dye molecules and on the length of the primitive unit cell. As an example, pyronine and oxonine (length ≈ 15 Å) in zeolite L ($|c| = 7.5$ Å) require two primitive cells per molecule, therefore u is equal 2. The sites form a new Bravais lattice with the primitive vectors a, b and $u \cdot c$.

(b)   There exist two types of sites. The first one can be occupied with dye molecules, we mark it with small letters. The second type, marked with capital letters, are reserved for
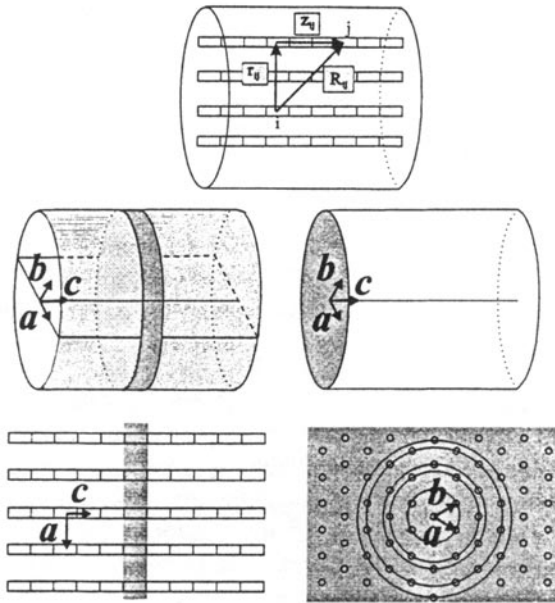
Figure 6. Geometrical arrangement of the antenna. The sites are marked by rectangles. Top: Definition of the distance R_{ij} r_{ij} and z_{ij} between sites i and j. Left: Cut through the center of the cylindrical microcrystal along a and c. The sites of the shaded area belong to one slab. Right: Cut vertical to c. The channels indicated by circles are arranged in rings around the central channel as a consequence of the hexagonal symmetry[10].

traps. Per microcrystal, the number of sites available for dye molecules is i_{max} and the number of sites available for traps is I_{max}. Both types of sites have the same geometrical properties. All dye molecules in sites i are assumed to be identical. This is realized by averaging over the thermal distribution. The same is valid for traps.

(c) Only dye molecules with a large electronic transition moment are taken into account. This means that the $S_1 \leftarrow S_0$ transition is of $\pi \leftarrow \pi$ type. We assume that the radiationless energy transfer between excited and unexcited molecules can be described by the dipole-dipole mechanism, the so-called Förster mechanism.

(d) The dye molecules are chosen such that their long axis coincides with the channel axes c. Hence, their short axes can occupy all directions perpendicular to c. We discuss cases where the relevant electronic transition dipole moment of the dye molecules coincides with their long axes. Therefore, both absorbed and emitted photons flow perpendicular to the c axis of the microcrystals.

(e) Each site i is occupied with the same probability p_i by a dye molecule. The occupation probability p_i is equal to the ratio between the occupied and the total number of sites. In cases where cationic dye molecules are intercalated by ion exchange, p_i is proportional to the exchange degree θ, which is defined as the ratio of dye molecules and exchangeable cations[36]. $[K^+]_z$ is the number of exchangeable cations per unit cell and the relation between the exchange degree θ and the occupation probability p_i is given by $p_i = \dot{u} [K^+]_z \theta$. The occupation probability p_1 of sites I is treated in an analogous way.

(f) Each site i of a given microcrystal has the same probability P_i to be occupied by an excited molecule, immediately after excitation with a Dirac pulse. The excitation probability P_i of site i is the ith element of a vector P which we call distribution of the excitation among the sites. We restrict the discussion to the low intensity case in which at maximum one dye molecule per microcrystal is in an electronically excited state. This means that intensity dependent processes such as e.g. stimulated emission do not occur.
(g) We do not consider radiationless decay pathways of the excited dye molecules. This would be easy to include but we are interested in dye molecules with a luminescence quantum yield of one or close to one. Pyronine and oxonine are examples which fulfil this condition well[9]. Self-absorption and reemission processes are of minor importance for the experimental conditions envisaged. They are therefore not discussed.

A $0.1\,\mu$m large zeolite L microcrystal with equal length and diameter ($l_{cyl} = 2.r_{cyl}$) contains about 750 parallel channels. Each channel consists of 134 unit cells. Dye molecules with a size like pyronine and oxonine occupy two unit cells ($u = 2$). This means that up to 67 dye molecules find place in one channel. Such a microcrystal can contain up to 50250 dye molecules. An impression on the rate of energy migration in such a system is provided in figure 7. It contains two kinds of information. We show in
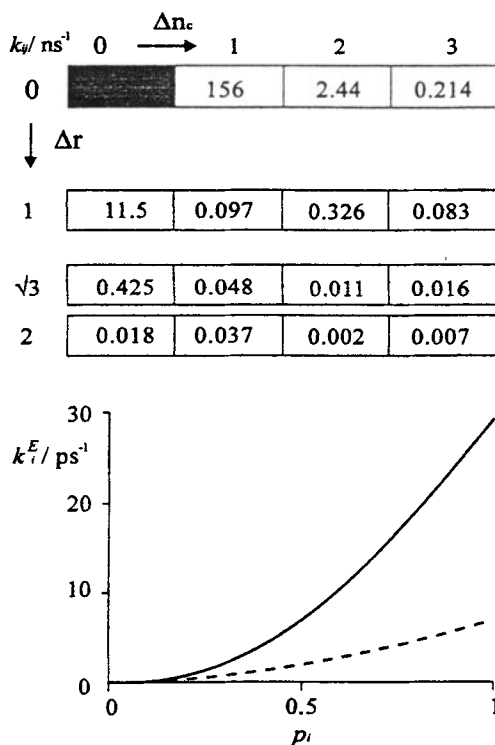

Figure 7. Rate constants for different situations. Top: Energy transfer rate constants k_{ij}, in units of $10^9\,\text{s}^{-1}$, for jumps from the shaded site i to neighbour sites j for $p_i = 0.25$ and $J_{ij} = 1.05 \cdot 10^{-13}\,\text{cm}^3\text{M}^{-1}$ Bottom: Depopulation rate constant k_i^E/ps of a site i as a function of the occupation probability p_i for $J_{ij} = 4.4 \cdot 10^{-13}\,\text{cm}^3\text{M}^{-1}$ (solid) and for $J_{ij} = 1.05 \cdot 10^{-13}\,\text{cm}^3\text{M}^{-1}$ (dashed).

the upper part individual rate constants k_{ij} from the starting site which is shaded to a representative selection of neighbour sites and in the lower part the energy migration constant k_i^E as a function of the occupation probability p_i. Energy transfer to the nearest neighbours along the channel axes, is by far, the most probable event. With increasing distance z_{ij} the individual rate constants k_{ij} for energy transfers decrease strongly. The reason for this is the pronounced distance dependence of the dipole-dipole interactions. Energy transfer to the nearest neighbours perpendicular to the channel axes is much less probable than along the channel axes. This difference is caused mainly by the orientation factor, which is strongly different for this two transitions, and not so much by the only slightly larger distance. We observe for the same reason that the rate constant for the transition along the vector $(\Delta n_a, \Delta n_c) = (1, 1)$ is much smaller than along the vector $(\Delta n_a, \Delta n_c) = (1, 2)$, although the distance for the latter transition is larger.

All rate constants k_{ij} are proportional to the square of the occupation probability p_i^2 and to the spectral overlap J_{ij}. The ratio between the different rate constants is therefore not affected by these parameters and any sum of rate constants k_{ij} shows the same proportionalities. The square dependence on the occupation probability of the energy migration constant k_i^E, which is the sum of the rate constants k_{ij} of energy transfers from site i to any site j of the microcrystal, is documented in the lower part of figure 7. Its value is significantly larger than $0.2\,\text{ps}^{-1}$ even at rather low occupation probabilities p_i. The energy migration constant in the antenna system of green photosynthetic bacterium *Chloroflexus aurantiacus* was reported to be $0.2\,\text{ps}^{-1}$[38].

Energy migration along the channel axes can be expressed as energy transfer from one slab to another. Analogously, energy migration perpendicular to it can be expressed as energy transfer between the channels. The rate constants reported in figure 8 for transitions between slabs, kz_{ij}, and between channels, kr_{ij}, have been calculated for the same occupation probability and the same spectral overlap as used for figure 7 (top). The rate constants between slabs are symmetrical, which mean $kz_{ij} = kz_{ji}$, and the kr_{ij} are the same for all channels sitting on the same circle around the shaded channel. Energy transfer to the next neighbour slabs is about 18 times more probable than to any other slabs. The rate constant for transitions between neighbour slabs is close to that for transitions between neighbour sites inside one channel. This means that energy migration along the channel axes runs predominantly inside of the same channel simply from one site to its nearest next neighbour. Energy migration perpendicular to the channel axes is much slower. It occurs predominantly between nearest next neighbour sites inside of the same slab.

We have shown that it is convenient to distinguish between different types of trapping[10]. They are named according to the position of the traps. *Front trapping* $T_F(t)$ refers to traps positioned only on the front side of the cylindrical microcrystals. Thus, they are found in the slab $n_c = 0$. *Front-back trapping* $T_{FB}(t)$ refers to traps on the front and to traps on the back positioned in the slab $n_c = 0$ and $n_c = n_c^{max}$, respectively. *Coat trapping* $T_C(t)$ refers to traps positioned on the coat of the cylinder, this means in the outermost channels having a distance to the central channel between $r_{max} - |a|$ and r_{max}. *Axial trapping* $T_A(t)$ refers to traps located in the central channel. Finally, *point trapping* $T_P(t)$ refers to a single trap positioned at the centre of the front side. All this trapping types reflect symmetry aspects of the cylinder investigated. Front-back trapping and front trapping are governed by energy migration along c while coat trapping and axial trapping are governed by energy migration perpendicular to it. Point trapping depends on both directions of energy migration.
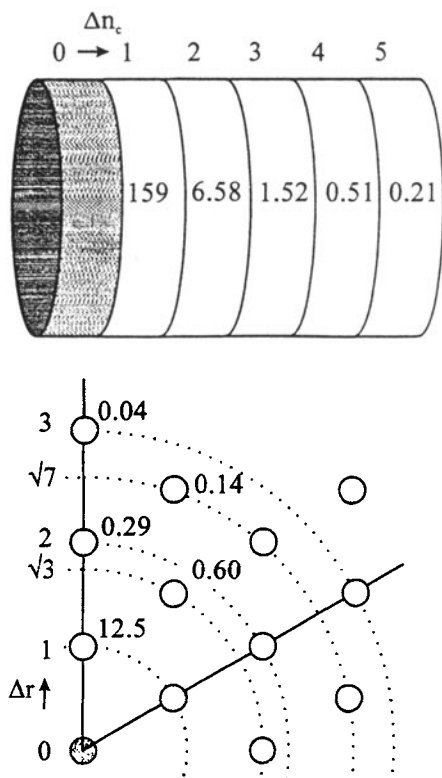
Figure 8. Rate constants for $J_{ij} = 1.05 \cdot 10^{-13} \, \text{cm}^3 \text{M}^{-1}$ and $p_i = 0.25 \cdot \Delta r$ is the distance between the channels in units of the shortest distance. Δn_c numbers the slabs with respect to the initial one. Top: Rate constants kz_{ij} for energy transfer from the shaded slab to the neighbour slabs j. Bottom: Rate constants kr_{ij} for energy transfer from the shaded channel to the neighbour channels j.

An important result we have obtained is summarized in table 1 where the *front trapping efficiency* $T_{F\infty}$ observed at infinite time after the excitation of a dye in antenna is reported as a function of the size of the microcrystal for two different occupation probabilities and two spectral overlaps. It shows that nearly quantitative trapping efficiencies are feasible in well designed system.

5. Conclusions

We have focused on three problems, the water oxidation in absence of an externally added potential, the charge transport in an organized microporous media and the transport of excitation energy in an antenna system.

It is satisfactory that the very efficient photochemical oxygen evolution on AgCl/Ag$^+$ systems can be explained as a sequence of simple one electron steps. The excess of Ag$^+$ needed for efficient oxygen evolution is a surface effect. The reduced silver species must be oxidized to make the photochemical water oxidation useful for solar energy conversion. It is not difficult to reoxidize the photochemically produced Ag^0 completely to Ag$^+$. It is, however, difficult to design a completely reversible and stable

Table 1. Front trapping efficiency $T_{F,\infty}$ and fluorescence quantum yield Φ_F for different cylinder lengths l_{cyl}, two different occupation probabilities p_i and two different spectral overlaps J_{ij}[10].

$l_{cyl}/$nm	P_i	$T_{F,\infty}$ $J_{ij}=1\cdot10^{-13}\text{cm}^3$ M^{-1}	Φ_F	$T_{F,\infty}$ $J_{ij}=4\cdot10^{-13}\text{cm}^3$ M^{-1}	Φ_F
50	0·25	0·62	0·38	0·86	0·14
100		·35	0·65	0·64	0·36
150		0·23	0·77	0·48	0·53
200		0·17	0·83	0·38	0·62
250		0·14	0·86	0·31	0·69
50	1	0·96	0·04	0·99	0·01
100		0·87	0·13	0·96	0·04
150		0·77	0·23	0·93	0·07
200		0·69	0·31	0·9	0·1
250		0·62	0·38	0·86	0·14

system. Two complementary approaches can be tried. One of them is to design a photo electrochemical cell in which the reduced silver is reoxidized electrochemically and in which hydrogen is evolved at an appropriate counter-electrode. The other one is to realize a completely reversible device by dividing it into an oxidative and a reductive half cell via a membrane. Zeolite based systems appear to be attractive for both approaches.

Zeolite microcrystals can act as hosts for supramolecular organization of clusters, complexes and molecules. They offer possibilities to design precise and reversible functionalities which have the potential to become useful for solar energy conversion. Arranging zeolite microcrystals as dense monograin layers of good quality on different types of substrates allows us to achieve specific properties. Three functionalities are of special importance: intrazeolite ion transport, intrazeolite charge transport and intrazeolite excitation energy transport. The zeolite acts as a host in each case.

Favourable conditions for an antenna device are highly concentrated monomeric dye molecules with a large Förster energy transfer radius and a high luminescence quantum yield in an ideal geometrical arrangement of optimal size. This can be realized by enclosing dyes inside of a microporous material in a way that the volume of the cages and channels is able to uptake monomers only but not aggregates. Zeolites bearing linear channels running through a whole microcrystal allow the formation of highly anisotropic dye assemblies. We have found that they can lead to nearly quantitative trapping efficiencies and that they bear the potential for becoming useful in solar energy conversion.

References

1. Balzani V, Campagna S, Denti G, Juris A, Serroni S and Venturi M 1995 *Solar Energy Mater. Sol. Cells* **38** 159
2. Bücher H, Drexhage K H, Fleck M, Kuhn H, Möbius D, Schäfer F P, Sondermann J , Sperling W, Tillmann P and Wiegand J 1967 *Mol. Crystals* **2** 199
3. Tributsch H, Proc. IPS-10, Tian Z W and Cao Y 1993 (eds.) *Intern. Academic Publishers, Beijing, China*, 235
4. Bignozzi C A, Argazzi R, Schoonover J R, Meyer G J and Scandola F 1995 *Solar Energy Mater. Sol. Cells* **38** 187
5. Amouyal E 1995 *Solar Energy Mater. Sol. Cells* **38** 249
6. Bard A J and Fox M A 1995 *Acc. Chem. Res.* **28** 141
7. Beer R, Binder F and Calzaferri G 1992 *Photochem. Photobiol. A: Chemistry* **69** 67; Calzaferri G, Hug S, Hugentobler T and Sulzberger B 1984 *ibid.* **26** 109; Sulzberger B and Calzaferri G 1982 *ibid.* **19** 321
8. Pfanner K, Gfeller N and Calzaferri G 1996 *J. Photochem. Photobiol. A: Chemistry* **95** 175
9. Binder F, Calzaferri G and Gfeller N 1995 *Sol. Energy Mater. Sol. Cells* **38** 175; Binder F, Calzaferri G and Gfeller N 1995 *Proc. Ind. Acad. Sci. (Chem. Sci.)* **107** 753
10. Gfeller N and Calzaferri G submitted for publication.
11. Riggs-Gelasco P J, Mei R, Yocum Ch F and Penner-Hahn J E 1996 *J. Am. Chem. Soc.* **118** 2387; Wieghrdt K 1994 *Angew. Chem.* **106** 765
12. Schaaf L J, 1992 Out of the Shadows: Herschel, Talbot and the Invention of Photography. Yale University Press, New Haven & London
13. Calgaferri G, Gfeller N and Pfanner K 1995 *J. Photochem. Photobiol. A: Chemistry* **87** 81
14. Ware M J 1995 IS&T's 48th Annual Conference Proceedings, Washington DC, May 7–11, p. 86.
15. Baur E and Rebmann A 1921 *Helv. Chim. Acta,* **4** 256
16. Vogel H 1863 *Ann. Phys.* **119** 497
17. Calzaferri G and Spahni W 1986 *J. Photochem . Photobiol. A: Chemistry* **32** 151; Beer R, Calzaferri G and Spahni W 1988 *Chimia* **42** 134
18. Metzner H and Fischer K 1974 *Photosynthetica* **8** 257; Metzner H, Fischer K and Lupp G 1975 *ibid.* **9** 327
19. Chandrashekharan K and Thomas J K 1983 *Chem. Phys. Lett.* **97** 357
20. Taube H and W. C. Bray 1940 *J. Am. Chem. Soc.* **62** 3357
21. Saladin F, Kamber I, Pfanner K and Calzaferri G to be submitted.
22. Calzaferri G, in Tian Z W and Cao Yi 1993 (eds), Proceedings of the 9th International Conference on Photochemical Conversion and Storage of Solar Energy, IPS-9, International Academic Publishers, Beijing, 141–157
23. Wöhrle D and Schulz-Ekloff G 1994 *Adv. Mater.* **6** 875; Caro J, Marlow F and Wübbenhorst M 1994 *Adv. Mater.* **6** 413; Schüth F 1995 *Chemie i. u. Zeit* **29** 42
24. Dutta P K, Borja M and Lendney M 1995 *Sol. Energy Mater. Sol. Cells* **38** 239
25. Lainé P, Seifert R, Giovanoli R and Calzaferri G, submitted for publication.
26. Lainé P, Lanz M and Calzaferri G 1996 *Inorg. Chem.* **35** 3514
27. Müller B R and Calzaferri G 1996 *J. Chem. Soc., Faraday Trans.* **92** 1633
28. Calzaferri G, Proceedings Taylor-Made Silicon-Oxygen Compounds, From Molecules to Materials, Bielefeld, Sept. 3–5, 1995, Ed. Jutzi, P.; Corriu R. 149–169.
29. Rálek M, Jiru P, Grubner O and Beyer H 1962 *Collect. Czech. Chem. Commun.* **27** 142
30. Sun T and Seff K 1994 *Chem. Rev.* **94** 857
31. Calzaferri G, Kunzmann A, Lainé P and Pfanner K 1995 IS&T's 48th Annual Conference Proceedings, Washington DC, May 7–11, p. 318
32. Kunzmann A, Rytz R and Calzaferri G, to be published
33. Calzaferri G, Lanz M and Li J W 1995 *J. Chem. Soc., Chem. Commun.* 1313
34. Kühlbrandt W and Wang D N 1991 *Nature,* **350** 131
35. Meier M W and Olson D H 1988 *Atlas of Zeolite Structure Types, Buttherworth: Stoneham, MA*, 1988.
36. Calzaferri G and Gfeller N 1992 *J. Phys. Chem.* **96** 3428

37. Ernst S and Weitkamp J 1994 *Catal. Today* **19** 27; Tsapatsis M, Tatsuya O, Lovallo M and Davis M E 1995 *Mat. Res. Soc. Symp. Proc.* **371** 21
38. Savikhin S, Zhu Y, Blankenship R E and Struve W S 1996 *J. Phys. Chem.* **100** 3320